第 30 卷 第 11 期 催 化 学 报 2009 年 11 月
Vol. 30 No. 11 *Chinese Journal of Catalysis* November 2009

文章编号: 0253-9837(2009)11-1091-05 **研究论文:** 1091~1095

SBA-15 的硅烷化对钴基催化剂费-托合成性能的影响

闪媛媛, 刘光荣, 李金林

中南民族大学催化材料科学湖北省暨国家民委-教育部共建重点实验室, 湖北武汉430074

摘要: 以未硅烷化和硅烷化的SBA-15为载体,采用满孔浸渍法制备了钴基费-托合成催化剂,通过元素分析、N_2吸附-脱附、X射线衍射、H_2程序升温还原、H_2程序升温脱附以及氧滴定等手段对催化剂进行了表征. 催化剂的费-托合成活性测试在固定床反应器上进行. 研究表明,对于SBA-15硅烷化后制备的催化剂,金属钴与载体之间的相互作用降低,氧化钴的还原度增加. 随着三甲基氯硅烷用量的增加,三甲基硅基的表面覆盖度增加,钴的晶粒直径增大. 硅烷化后的催化剂的高活性归因于高的还原度,而C_{5+}选择性的增加则归因于钴晶粒直径的增大.

关键词: 硅烷化; SBA-15; 钴基催化剂; 费-托合成; 三甲基硅基

中图分类号: O643 **文献标识码:** A

Effect of Silylation of SBA-15 on Its Supported Cobalt Catalysts for Fischer-Tropsch Synthesis

SHAN Yuanyuan, LIEW Kongyong, LI Jinlin*

Key Laboratory of Catalysis and Materials Science of the State Ethnic Affairs Commission and Ministry of Education, South-Central University for Nationalities, Wuhan 430074, Hubei, China

Abstract: Cobalt catalysts supported on unsilylated and silylated SBA-15 were prepared by incipient wetness impregnation and characterized by elemental analysis, N_2 adsorption-desorption, X-ray diffraction, H_2 temperature-programmed reduction, H_2 temperature-programmed desorption, and oxygen titration. Their catalytic properties for Fischer-Tropsch synthesis were evaluated in a fixed-bed reactor. The results show that the interaction between cobalt and the support was decreased, and the reducibility of the cobalt oxide species was more facile on the silylated Co/SBA-15 catalyst. With increasing $(CH_3)_3SiCl$ loading, the surface coverage of the trimethylsilyl group increased, and the cobalt cluster size was larger. The higher activity of the silylated 10%Co/SBA-15 catalysts was ascribed to its improved reducibility. The increase in selectivity for C_{5+} hydrocarbons was attributed to the increase in cobalt cluster size.

Key words: silylation; SBA-15; cobalt-based catalyst; Fischer-Tropsch synthesis; trimethylsilyl

Fischer-Tropsch synthesis (FTS) is used to convert carbon monoxide and hydrogen into transportation fuels and chemicals [1]. The synthetic fuels produced by FTS have high molecular weights and are straight chain hydrocarbons that can be used as blending stock for transportation fuels derived from crude oil [2]. Cobalt-based FTS catalysts have been widely studied because of their high conversion, high selectivity for heavy hydrocarbons, low water-gas shift activity, and comparatively low price [3].

In principle, the FTS activity of supported cobalt is proportional to the number of surface Co^0 sites on the reduced catalysts. Cobalt dispersion and reducibility are believed to be the important parameters that affect the number of surface cobalt sites, and thus the overall catalytic performance [4,5]. Typically, the reducibility of supported cobalt oxide can be made more facile by the addition of small amounts of noble metals and transition metals, such as Pt [6], Re [7], Ru [8], and Zr [9]. Some advanced methods that can improve the reducibility of supported cobalt catalysts have been developed recently [10,11].

Cobalt is usually supported on conventional supports such as Al_2O_3, TiO_2, SiO_2, and ZrO_2 for the FTS reaction [12–14]. SBA-15 is a highly ordered mesoporous molecular sieve with a narrow pore size distribution of 3–30 nm and

Received date: 14 April 2009.
***Corresponding author.** Tel: +86-27-67843016; Fax: +86-27-67842752; E-mail: lij@mail.scuec.edu.cn
Foundation item: Supported by the National Natural Science Foundation of China (20590360 and 20773166).
English edition available online at ScienceDirect (http://www.sciencedirect.com/science/journal/18722067).

large surface area (600–1000 m^2/g) [15]. SBA-15 has thicker pore walls and higher hydrothermal stability than other silica-based mesoporous materials such as MCM-41. These features make it suitable for use as a support material [16]. It has been suggested that surface silanol groups (SiOH) on siliceous materials can interact with cobalt oxides [17,18]. The resulting compounds were difficult to reduce at low temperatures. Kim et al. [10] studied the performance of catalysts supported on SBA-15 silylated by $(CH_3)_3SiSi(CH_3)_3$ (HMDS) and found that the silylation enhanced the reducibility of cobalt oxides and increased the FTS activity. Martínez et al. [19] synthesized cobalt metal nanoparticles in the core of reverse micelles and supported the nanoparticles on ITQ-2 silylated by HMDS. They found that this preparation approach did not have the dispersion-reducibility dependence of very small cobalt particles, and these modified carriers led to increased metal dispersion and consequently increased activity.

In the present work, we studied silylated SBA-15- supported cobalt catalysts for FTS. The catalysts were prepared by the incipient wetness impregnation method and characterized by elemental analysis, N_2 adsorption-desorption, X-ray diffraction (XRD), H_2 temperature-programmed reduction (H_2-TPR), H_2 temperature-programmed desorption (H_2-TPD), and oxygen titration. The effect of the silylation of SBA-15 on the activity and selectivity of the FTS reaction was investigated.

1 Experimental

1.1 Catalyst preparation

SBA-15 was synthesized according to a reported procedure [15]. In a typical synthesis, 10 g of P123 ($EO_{20}PO_{70}EO_{20}$, M_{AV} = 5800, AR, Aldrich) was stirred with 350 ml of 2 mol/L HCl solution at 35 ºC until completely dissolved. This was followed by the dropwise addition of 22.5 g of TEOS (tetraethylorthosilicate, AR, Sinopharm Chemical Reagent Co., Ltd). After stirring at 35 ºC for 24 h, the mixture was charged into a polytetrafluoroethylene bottle and then heated at 100 ºC for 24 h. The precipitate was thoroughly washed with deionized water, dried at room temperature, and then calcined in air at 550 ºC for 6 h.

The procedure for the silylation of SBA-15 was as follows [20]. The synthesized SBA-15 was evacuated at 120 ºC for 6 h to remove the residual water. The SBA-15 (2 g) was dispersed in anhydrous toluene (160 ml). Then $(CH_3)_3SiCl$ (TMCS, AR, Alfa Aesar) was added slowly under stirring. Each mixture was stirred at 80 ºC for 24 h under N_2 atmosphere. The samples were then filtered and washed with toluene and ethanol. Three different amounts of silylation were performed by adding 2, 10, and 20 ml of TMCS into the suspension.

The cobalt catalysts supported on silylated and unsilylated SBA-15 (10% cobalt) were prepared by incipient wetness impregnation using an ethanol solution of cobalt nitrate. After impregnation, the catalysts were dried at 120 ºC for 12 h and calcined in a flow of air at 450 ºC for 5 h. The samples were named 10%Co/SBA-15-SX with X = 1, 5, and 10, where X denotes the amount (ml) of TMCS added per gram of SBA-15.

1.2 Support and catalyst characterization

The carbon contents of the silylated samples were determined with a Vario EL III elemental analyzer with a thermal conductivity detector (TCD). The surface coverage of the trimethylsilyl group was calculated using the equation: surface coverage = $(1/3\times n_c\times N\times A_{TMS}\times(10^{-9})^2)/A_{catal}$, where n_c is the mole number of carbon on the surface of support, N is Avogadro's Number, A_{TMS} is the area of trimethysilyl group per molecule [21], and A_{catal} is the surface area of catalyst.

N_2 adsorption-desorption isotherms were measured at –196 ºC using a Quantachrome Autosorb-1 analyzer. Prior to the measurement, the samples were degassed at 200 ºC for 6 h. The surface area was calculated from the BET equation, and the pore size distribution and pore volumes were determined from the desorption branch of the isotherms using the Barrett-Joyner-Halenda method.

Small-angle and wide-angle XRD patterns were obtained with a Bruker D8 power diffractometer using nickel-filtered Cu K_α radiation (λ = 0.154056 nm). The scan ranges were 0.5°–4° and 20°–80° with 0.002° and 0.016° steps, respectively. Crystallite phases were determined by comparing the diffraction patterns with those in the standard JCPDS powder diffraction file.

H_2-TPR experiments were performed with a Zeton Altamira AMI-200 unit with a TCD. About 0.04 g of the calcined catalyst was placed in a U-shaped tubular quartz reactor and purged with 30 ml/min Ar at 150 ºC for 1 h to remove water, and then cooled to 50 ºC. Then 10%H_2-90%Ar was introduced to the catalyst at a flow rate of 30 ml/min while the temperature was increased at a rate of 10 ºC/min from 50 to 800 ºC and held at 800 ºC for 0.5 h.

H_2-TPD was also performed using the Zeton Altamira AMI-200 unit. The catalyst (0.15 g) was reduced by H_2 at 450 ºC for 12 h and cooled under H_2 flow to 100 ºC. The sample was held at 100 ºC for 1 h under Ar flow to remove weakly bonded physisorbed species. The temperature was increased slowly to 450 ºC, and the catalyst was held at this temperature under flowing argon to desorb the remaining chemisorbed H_2 until the TCD signal returned to the baseline. Oxygen pulse reoxidation was also performed with the Zeton Altamira AMI-200 unit. After the H_2-TPD, the sample

was reoxidized at 450 ºC by oxygen pulses into a helium carrier. After oxidation of the cobalt metal particles was completed, the number of moles of oxygen consumed and the percentage reduction were calculated assuming that Co^0 was reoxidized completely to Co_3O_4.

The calculation of the dispersion and average cluster size assumed that the Co:H stoichiometry was 1:1. The cobalt metal cluster size was estimated assuming spherical cobalt cluster morphology [22]. The uncorrected cluster size and dispersion were calculated based on the total cobalt contained in the sample, and the corrected cluster size and dispersion were reported by reduction percentage. The formula for the calculation has been described previously [23].

1.3 Fischer-Tropsch synthesis reaction

The performance of the catalysts for FTS was tested in a fixed-bed reactor (i.d. = 12 mm). The sample (0.4 g) diluted with 5.0 g of carborundum was placed in the reactor. Prior to the catalytic measurements, the catalysts were reduced at 450 ºC and atmospheric pressure by a flow of high purity H_2 through the reactor at 6 NL/(h·g). After 10 h reduction, the reactor temperature was decreased to 100 ºC under H_2 flow. Synthesis gas with CO/H_2=1:2 at 8 SL/(h·g) was then introduced, and the pressure was increased slowly to 1.5 MPa. The temperature was increased to 215 ºC over 20 h, and the reaction was carried out at 215 ºC. The products were collected in a heated trap (100 ºC) and a cold trap (–2 ºC) in sequence. The outlet gases were analyzed online with an Agilent 300 GC. Activity was reported as CO conversion (X(CO)). C_{5+} selectivity was calculated by subtracting the amount of C_1–C_4 hydrocarbons in the product gas mixture from the total mass balance.

2 Results and discussion

2.1 Structure of the support and catalyst

The carbon content and surface coverage of the trimethylsilyl group are reported in Table 1. It can be seen that the surface coverage of the trimethylsilyl group on the silylated catalysts increased with increasing TMCS loading.

The N_2 adsorption-desorption isotherms for SBA-15 and the catalysts are shown in Fig. 1. The pure-silica SBA-15 sample displayed a typical IV isotherm with a H1 hysteresis loop. There was a sharp increase in the adsorbed amount of N_2 in the relative pressure range p/p_0 = 0.6–0.8. This is characteristic of highly ordered mesoporous materials. For all the Co/SBA-15 catalysts, the N_2 adsorption isotherms were similar to that of the original SBA-15. These indicate that the parent mesoporous structure was maintained after silylation and cobalt loading. The BET surface area, pore volume, and average pore diameter are given in Table 1. The BET surface area and pore volume of SBA-15 decreased after silylation and then decreased further after cobalt impregnation, which can be attributed to the entry of organic groups and cobalt species into the pores of the support, respectively.

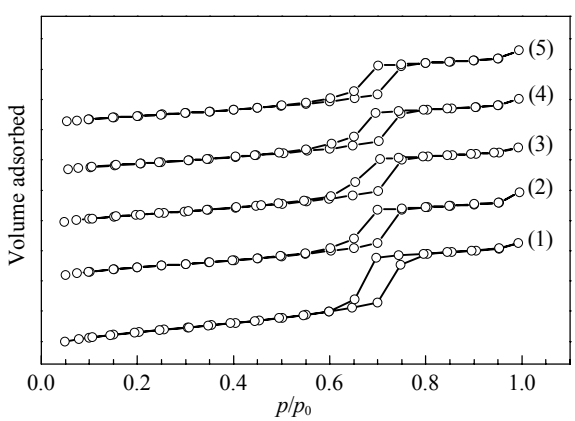

Fig. 1. N_2 adsorption-desorption isotherms of SBA-15 and 10%Co/SBA-15 catalysts with different amounts of silylation. (1) SBA-15; (2) 10%Co/SBA-15; (3) 10%Co/SBA-15-S1; (4) 10%Co/SBA-15-S5; (5) 10%Co/SBA-15-S10.

Figure 2 shows the XRD patterns of the SBA-15 and Co/SBA-15 catalysts. It can be seen from Fig. 2(a) that all the patterns had three well-resolved peaks at 2θ values between 0.9° and 2°, which can be indexed as the (100), (110), and (200) diffraction planes due to the 2-D hexagonal structure of the original SBA-15. However, compared with the intensity of the (100) diffraction peak of SBA-15, those of the catalysts containing cobalt decreased. This could be caused by a partial collapse of the periodic mesoporous structure during cobalt loading. As shown in Fig. 2(b), the

Table 1 N_2 adsorption-desorption data of SBA-15 and 10%Co/SBA-15 catalysts

Sample	Amont of TMCS[a] (ml/g)	C content (%)	Surface coverage (%)	A_{BET}/(m^2/g)	V_{BJH}/(cm^3/g)	d_{BJH}/nm
SBA-15	—	—	—	844.1	1.286	6.5
10%Co/SBA-15	—	—	—	661.8	1.060	6.5
10%Co/SBA-15-S1	1	1.171	14.93	624.5	0.9635	6.2
10%Co/SBA-15-S5	5	1.434	20.81	548.6	0.9034	6.5
10%Co/SBA-15-S10	10	1.472	23.47	499.3	0.8918	6.5

[a] Amount of TMCS added per gram of SBA-15.

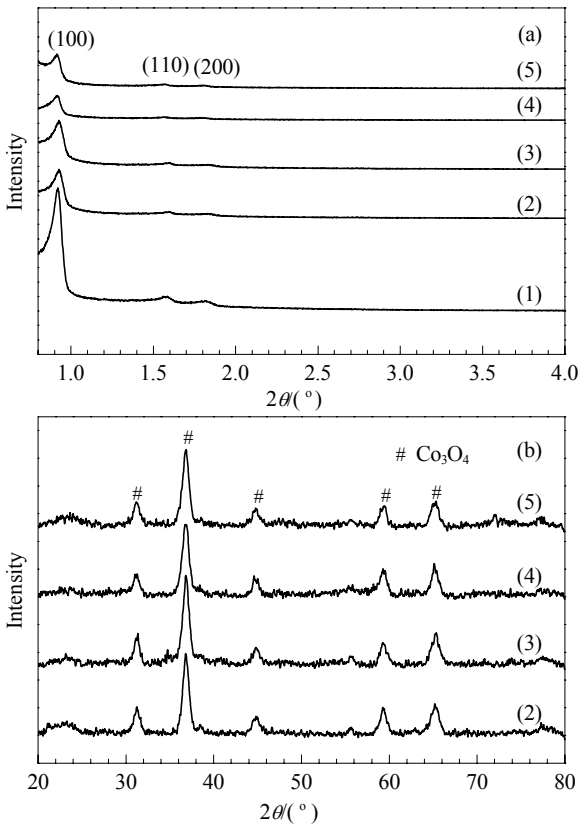

Fig. 2. XRD patterns of the samples. (a) Small-angle; (b) Wide-angle. (1) SBA-15; (2) 10%Co/SBA-15; (3) 10%Co/SBA-15-S1; (4) 10%Co/SBA-15-S5; (5) 10%Co/SBA-15-S10.

diffraction peaks at 31.2°, 36.8°, 44.8°, 59.4°, and 65.3° corresponded to the face-centered cubic spinel of crystalline Co_3O_4 (JCPDS PDF No. 42-1467). It is noteworthy that Co_3O_4 was the primary crystalline cobalt species present after impregnation and calcination.

2.2 Catalyst reducibility

Figure 3 shows the TPR profiles of the unsilylated and silylated Co/SBA-15 catalysts. The TPR profiles show three main reduction peaks centered at 305, 442, and 626 ºC. According to the in-situ XRD data in our previous study [24], the low temperature reduction region at 216–323 ºC can be attributed to the reduction of Co_3O_4 to CoO. The second peak at 323–550 ºC corresponded to the subsequent reduction of CoO to Co^0. For the unsilylated Co/SBA-15 catalyst, the broad peak at 550–740 ºC can be assigned to the reduction of barely reducible cobalt silicate (Co_2SiO_4) formed by a strong interaction between cobalt and the support [25]. After silylation of the SBA-15 surface, the high temperature reduction peak intensity decreased, indicating that the strong interaction between the cobalt species and surface SiOH groups decreased. Kim et al. [10] reported that the intensity of the peak at above 570 ºC increased with the loading of HMDS, while in the present study, the peak intensity at above 550 ºC decreased.

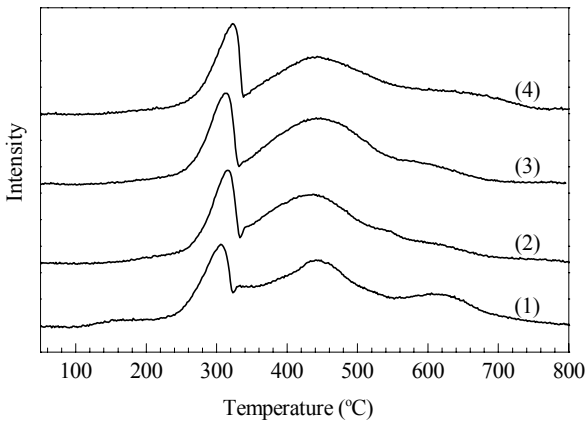

Fig. 3. H_2-TPR profiles for unsilylated and silylated catalysts with different amounts. (1) 10%Co/SBA-15; (2) 10%Co/SBA-15-S1; (3) 10%Co/SBA-15-S5; (4) 10%Co/SBA-15-S10.

The results of H_2-TPD and O_2 titration are given in Table 2. With increased TMCS loading, the corrected cobalt dispersion decreased, the catalyst reducibility increased, and the corrected cobalt cluster size increased. The reason is probably because the silylation reagent TMCS has reacted with the hydroxyl groups prior to the impregnation of cobalt. This decreased the concentration of the surface SiOH groups, which resulted in a decrease in the interaction between the cobalt species and SBA-15. The decreased interaction led to more facile reducibility and reduced the cobalt metal particle size.

2.3 Fischer-Tropsch synthesis activity

The catalyst activity and selectivity for FTS are summarized in Table 3. It can be seen that the activity and selectiv-

Table 2 H_2-TPD and pulse oxidation results for unsilylated and silylated cobalt SBA-15 catalysts

Sample	H_2 desorbed (μmol/g)	O_2 uptaked (μmol/g)	Reducibility (%)	Catalyst dispersion (%)		Metal cluster diameter (nm)	
				Uncorrected	Corrected	Uncorrected	Corrected
10%Co/SBA-15	37.5	193.0	16.98	4.43	26.27	23.3	3.51
10%Co/SBA-15-S1	32.3	288.4	25.37	3.81	15.02	27.1	6.88
10%Co/SBA-15-S5	34.6	356.9	31.39	4.07	12.97	25.3	7.94
10%Co/SBA-15-S10	35.7	395.7	34.80	4.21	12.10	24.3	8.46

Table 3 FTS performance of cobalt SBA-15 catalysts with different amounts of silylation

Sample	*X*(CO)/%	Hydrocarbon selectivity (%)				
		CH_4	C_2	C_3	C_4	C_{5+}
10%Co/SBA-15	12.30	11.39	0.54	5.22	6.07	76.78
10%Co/SBA-15-S1	17.19	9.70	0.59	3.77	5.01	80.94
10%Co/SBA-15-S5	18.46	8.24	0.35	3.63	4.37	83.41
10%Co/SBA-15-S10	20.40	7.56	0.36	3.50	4.10	84.48

Reaction conditions: 1.5 MPa, 215 ºC, CO:H_2 = 1:2, GHSV = 8 SL/(h·g).

ity of the catalysts were sensitive to the surface of the silica support. With increasing TMCS loading, the CO conversion increased, methane selectivity decreased, and C_{5+} hydrocarbon selectivity had a similar trend to the CO conversion.

It has been suggested that the cobalt catalyst activity for FTS was strongly dependent on catalyst reducibility. Khodakov et al. [11] found that the higher reducibility of larger cobalt particles formed in wider pore SBA-15 support led to a higher FTS reaction rate than could be obtained with the smaller pore MCM-41 support. Belambe et al. [26] reported that the FTS activity of Ru-promoted Co/Al_2O_3 decreased with catalysts calcined at a high temperature due to a decrease in the number of surface active sites for less reducible catalysts. In the present work, the reducibility of the catalysts increased, and this led to an increase in the FTS reaction activity with the silylated SBA-15-supported cobalt catalysts. This is in agreement with the conclusions of Khodakov et al. [11] and Belambe et al. [26]. The higher C_{5+} selectivity and lower CH_4 selectivity for the silylated cobalt catalysts were due to the larger cobalt particle size, which is consistent with the results of Co/γ-Al_2O_3 catalysts [27].

3 Conclusions

Cobalt catalysts supported on SBA-15 silylated by TMCS and their Fischer-Tropsch synthesis activity and selectivity were investigated. The structure of the original support was retained in the silylated SBA-15. Compared with the unsilylated cobalt catalyst, the silylated catalyst exhibited lower dispersion, higher reducibility, and larger cobalt cluster size. Improved catalysts with higher CO conversion and better C_{5+} hydrocarbon selectivity for Fischer-Tropsch synthesis were obtained.

References

1 Schulz H. *Appl Catal*, 1999, **186**: 3
2 Dai X P, Yu Ch Ch. *J Nat Gas Chem*, 2008, **17**: 17
3 Dry M E. *Catal Today*, 2002, **71**: 227
4 Panpranot J, Goodwin J G Jr, Sayari A. *J Catal*, 2002, **211**: 530
5 Iglesia E, Soled S L, Fiato R A. *J Catal*, 1992, **137**: 212
6 Li J L, Zhan X D, Zhang Y Q, Jacobs G, Das T, Davis B H. *Appl Catal A*, 2002, **228**: 203
7 Rygh L E S, Nielsen C J. *J Catal*, 2000, **194**: 401
8 Kogelbauer A, Goodwin J G Jr, Oukaci R. *J Catal*, 1996, **160**: 125
9 Feller A, Claeys M, van Steen E. *J Cata*l, 1999, **185**: 120
10 Kim D J, Dunn B C, Cole P, Turpin G, Ernst R D, Pugmire R J, Kang M, Kim J M, Eyring E M. *Chem Commun*, 2005: 1462
11 Khodakov A Y, Griboval-Constant A, Bechara R, Zholobenko V L. *J Catal*, 2002, **206**: 230
12 Jacobs G, Das T K, Zhang Y Q, Li J L, Racoillet G, Davis B H. *Appl Catal A*, 2002, **233**: 263
13 徐振刚, 罗伟, 王乃继, 肖翠微. 煤炭转化 (Xu Zh G, Luo W, Wang N J, Xiao C W. *Coal Conversion*), 2008, **31**(3): 92
14 Ji Y G, Zhao Zh, Yu Ch Ch, Duan A J, Jiang G Y. *Chem Ind Eng Progress*, 2007, **26**: 927
15 Zhao D Y, Huo Q S, Feng J L, Chmelka B F, Stucky G D. *J Am Chem Soc*, 1998, **120**: 6024
16 Huang B Y, Li X J, Ji Sh F, Lang B, Habimana F, Li Ch Y. *J Nat Gas Chem*, 2008, **17**: 225
17 Kubota Y, Ikeya H, Sugi Y, Yamada T, Tatsumi T. *J Mol Catal A*, 2006, **249**: 181
18 Zhang Y, Hanayama K, Tsubaki N. *Catal Commum*, 2006, **7**: 251
19 Martínez A, Prieto G. *J Catal*, 2007, **245**: 470
20 Zhang L X, Shi J L, Yu J, Hua Z L, Zhao X G, Ruan M L. *Adv Mater*, 2002, **14**: 1510
21 Corma A, Domine M, Gaona J A, Jord´a J L, Navarro M T, Rey F, Pérez-Pariente J, Tsuji J, McCulloch B, Nemeth L T. *Chem Commun*, 1998: 2211
22 Reuel R C, Bartholomew C H. *J Catal*, 1984, **85**: 63
23 Song D C, Li J L. *J Mol Catal A*, 2006, **247**: 206
24 Xiong H F, Zhang Y H, Liew K Y, Li J L. *J Mol Catal A*, 2008, **295**: 68
25 Martínez A, López C, Márquez F, Díaz I. *J Catal*, 2003, **220**: 486
26 Belambe A R, Oukaci R, Goodwin J G Jr. *J Catal*, 1997, **166**: 8
27 Borg Ø, Eri S, Blekkan E A, Storsæter S, Wigum H, Rytter E, Holmen A. *J Catal*, 2007, **248**: 89